International Journal of Research and Technology (IJRT)

International Open-Access, Peer-Reviewed, Refereed, Online Journal

ISSN (Print): 2321-7510 | ISSN (Online): 2321-7529

| An ISO 9001:2015 Certified Journal |

Fusion of MRI and Transcriptomic Signatures for Accurate Early Diagnosis of Alzheimer's Disease

Bhawana Purohit

Research Scholar, Shri Khushal Das University Hanumangarh, Rajasthan

Dr. Garima Bansal

Assistant professor, Shri Khushal Das University Hanumangarh, Rajasthan

ABSTRACT

Alzheimer Disease (AD) is a universal health issue whose proper therapeutic management has much reliance on its early and precise diagnosis. The existing methods of diagnosis are sophisticated but they tend to reveal the pathology when the neurons have been damaged to large extents. The research problem of this study is the investigation of the synergistic capability of structural MRI biomarkers and blood-based transcriptomic signatures in order to develop a multi-modal diagnostic model of early-stage AD detection. We examined cross-sectional data of 847 subjects (283 healthy controls, 284 mild cognitive impairment [MCI], 280 AD dementia) of the Alzheimer Disease Neuroimaging Initiative (ADNI) database. The combination of volumetric MRI measurements (hippocampal volume, entorhinal cortex thickness, ventricular volume) with blood-based transcriptomic signatures of neuroinflammatory (TSPO, GFAP, TREM2), oxidative stress (SOD1, CAT, GPX1), and tau-related (MAPT, EIF2AK2) gene expression was used. The implementation and validation of multi-modal machine learning models (Random Forest, Support Vector Machine, XGBoost) were carried out with the help of 5-fold cross-validation. Integrated MRI-transcriptomic model showed excellent diagnostic outcomes (AUC = 0.94, 95% CI: 0.91-0.96) than MRI-only (AUC = 0.86) and transcriptomic-only (AUC = 0.82) models. The strongest predictors were hippocampal volume (importance: 0.24) and GFAP expression (importance: 0.18). The model reached 89 and 91 sensitivity and specificity in differentiating MCI and controls respectively and had especially high rates in early-stage diagnosis. Combining neuroimaging biomarkers with transcriptomic biomarkers gives complementary data which dramatically increases the diagnosis accuracy of early AD patients. This multi-modern model provides an encouraging prospect of achieving precision medicine in AD management.

Keywords: Alzheimer Disease; MRI biomarkers; transcriptomics; multi-modal fusion, early diagnosis, neuroinflammation.

1. INTRODUCTION

AD is a neurodegenerative disease, the most common cause of dementia globally, and it is estimated that there are currently 50 million cases of AD and it is predicted that there will be over 150 million cases of AD by 2050 (Frironi et al., 2025; Porsteinsson et al., 2021). The AD pathological cascade starts decades prior to the development of clinical symptoms, which is a significant opportunity to implement early intervention that may possibly alter the disease progression (Jack et al., 2018; Jia et al., 2024).

The current pathophysiology of AD includes the presence of amyloid-2 deposition, hyperphosphorylated tau neurofibrillary tangles, neuroinflammation, oxidative stress, and dysfunction of the synapses (Firdous et al., 2024; Granzotto & Sensi, 2024). Although the amyloid cascade hypothesis keeps evolving, it continues to be the core of the knowledge on disease progression and growing evidence is that there are intricate interplays between various molecular pathways (Frisoni et al., 2022; Allen et al., 2018).

Modern diagnostic methods have gone a long way with cerebrospinal fluid (CSF) biomarkers, such as A beta 42, total tau, and phosphorylated tau (Blennow et al., 2015; Ossenkopke et al., 2022). Nevertheless, lumbar puncture is still invasive and is infeasible to screen a large population. Biomarkers in blood such as plasma p-tau181, p-tau217, and neurofilament light chain (NfL) have become promising options that have a strong association with cerebral pathology (Pacoova Dal Maschio et al., 2025; Quispialaya et al., 2023; Barthélemy et al., 2020).

Neuroimaging modalities have supplementary structural and functional data. Volumetry using MRI is able to display typical patterns of atrophy, especially in medial temporal lobe regions such as hippocampus and entorhinal cortex (Johnson et al., 2012; Frisoni et al., 2022). FDG-PET imaging is a capture of metabolic dysfunction, and amyloid and tau PET give direct visualization of the molecular pathology (Ossenkoppele et al., 2022; Jack et al., 2018).

Transcriptomic signatures represent changing cellular responses to dynamic pathology recorded through dynamic changes in gene expression. Neuroinflammatory biomarkers such as TSPO (activation of microglia), GFAP (astroglotrophic activity), and TREM2 (microglial functionality) obtain stable changes in the course of the disease (Roveta et al., 2024; Heneka et al., 2015). Early dysregulation is indicated by the activation of oxidative stress pathways via SOD1, CAT, and GPX1 (Balmuș et al., 2017), whereas tau-related genes such as MAPT indicate cytoskeletal pathology (Wang et al., 2012; Barbier et al., 2019).

The basic assumption behind this study is based on the hypothesis that MRI and transcriptomic biomarkers are complementary: structural neuroimaging will reflect the cumulative neurodegenerative impairment whereas transcriptomic signatures will represent ongoing pathology and therapeutic mechanisms. The combination of them can thus provide an earlier and more correct diagnosis compared to either of the two modalities.

2. METHODS

2.1 Study Population

The Alzheimer Disease Neuroimaging Initiative (adni.loni.usc.edu) database was used to obtain the data. Inclusion criteria included: (1) age 55-90 years of age; (2) 3T MRI baselines; (3) availed blood samples in transcriptomic study; (4) full clinical and neuropsychological evaluation. The criteria of exclusion were the presence of important neurological conditions other than AD, contraindications to MRI, and unstable health conditions.

The last group was 847 participants stratified into three diagnostic groups according to standard criteria (Jack et al., 2018): healthy controls (HC, n=283) with normal cognitive functioning; mild cognitive impairment (MCI, n=284) with objective cognitive impairment without

International Journal of Research and Technology (IJRT)
International Open-Access, Peer-Reviewed, Refereed, Online Journal
ISSN (Print): 2321-7510 | ISSN (Online): 2321-7529
| An ISO 9001:2015 Certified Journal |

functional decline; and AD dementia (AD, n=280) with NIA-AA probable AD dementia. Table 1 gives detailed demographic and clinical features.

Table 1. Demographic and Clinical Characteristics of Study Participants

Characteristic	Healthy Controls (n=283)	MCI (n=284)	AD Dementia (n=280)	p-value
Age (years), mean ± SD	72.4 ± 6.8	73.1 ± 7.2	74.2 ± 7.5	0.012
Sex (female), n (%)	148 (52.3)	128 (45.1)	136 (48.6)	0.21
Education (years), mean ± SD	16.2 ± 2.6	15.9 ± 2.8	15.4 ± 2.9	0.003
MMSE score, mean ± SD	29.1 ± 1.1	27.3 ± 1.8	22.4 ± 3.2	<0.001
CDR-SB, mean ± SD	0.03 ± 0.1	1.8 ± 0.9	5.2 ± 2.1	<0.001
APOE ε4 carriers, n (%)	71 (25.1)	126 (44.4)	158 (56.4)	<0.001
Hippocampal volume (mm^3), mean ± SD	3856 ± 412	3421 ± 458	2893 ± 521	<0.001
CSF Aβ42 (pg/mL), mean ± SD	1124 ± 286	892 ± 312	654 ± 278	<0.001
CSF p-tau181 (pg/mL), mean ± SD	52.3 ± 18.6	68.4 ± 24.2	89.7 ± 31.4	<0.001

Abbreviations: MCI, mild cognitive impairment; AD, Alzheimer's Disease; SD, standard deviation; MMSE, Mini-Mental State Examination; CDR-SB, Clinical Dementia Rating Scale Sum of Boxes; APOE, apolipoprotein E; CSF, cerebrospinal fluid.

2.2 MRI Acquisition and Processing

All participants underwent 3T MRI scanning using standardized ADNI protocols (http://adni.loni.usc.edu/methods/documents/mri-protocols/). T1-weighted structural images were obtained using magnetization-prepared rapid gradient-echo (MPRAGE) sequences as follows; TR/TE = 2300/2.98 ms, flip angle= 9o, voxel size= 1.0x1.0x1.2 mm -1.

Cortical reconstruction and volumetric segmentation were done using image processing (FreeSurfer 7.2, http://surfer.nmr.mgh.harvard.edu). The processing chain consisted of motion correction, non-brain tissue removal, Talairach transformation, subcortical white and deep gray

matter structure segmentation, intensity normalization, graywhite-boundary tessellation, and topology-correction-v3.

Primary regions of interest (ROIs) were chosen on the basis of previously determined AD vulnerability: volume of hippocampal, volume of entorhinal cortex, volume of parahippocampal gyrus, volume of amygdala, volume of inferior lateral ventricular, and volume of whole brain. All the volumetric data were standardized to the estimated total intracranial volume (eTIV) so that variation in head size could be corrected.

2.3 Transcriptomic Analysis

PAXgene RNA tubes were used to collect blood samples that were processed as per standardized procedures. The PAXgene Blood RNA Kit (Qiagen) was used to extract RNA and the quality was assessed using Agilent Bioanalyzer. RNA integrity samples whose RIN was greater than 7.0 were submitted to microarray analysis on Affymetrix Human Genome U219 arrays.

Raw data were subjected to normalisation and log2 transformation of multi-array average (RMA) which was robust. Quality control entailed checking the distribution of array intensities, use of principal component analysis to identify outliers and determination of housekeeping gene stability.

The selection of genes was based on literature review and dealt with three pathophysiological areas (Roveta et al., 2024; Firdous et al., 2024; Lashley et al., 2018):

Neuroinflammation panel: TSPO (microglial activation), GFAP (astrocyte activation), TREM2 (microglial function), CD33 (microglial regulation), IL1B (pro-inflammatory cytokine), TNF (pro-inflammatory cytokine), IL6 (pro-inflammatory cytokine), CX3CR1 (neuronal-microglial signaling), AIF1 (microglial activation) and C1QA (complement pathway).

Oxidative stress panel: SOD1 (superoxide dismutase), SOD2 (mitochondrial superoxide dismutase), CAT (catalase), GPX1 (glutathione peroxidase), GSR (glutathione reductase), TXN (thioredoxin), TXNIP (thioredoxin-interacting protein), NFE2L2 (NRF2 transcription factor), HMOX1 (heme oxygenase) and NQO1 (NAD(P)H quinone deh

Tau-associated panel: MAPT (tau protein), EIF2AK2 (PKR, tau kinase), GSK3B (tau kinase), CDK5 (tau kinase), MARK2 (microtubule affinity-regulating kinase), PPP1R1B (DARPP-32, phosphatase regulation), BIN1 (tau pathology modifier) and PTK2B (tau kinase).

2.4 Multi-Modal Fusion Approach

We came up with three modeling methods:

MRI-only model: Using 15 features of structural imaging such as regional volumes and cortical thickness measures.

Transcriptomic model alone: This model used 28 gene expression values of the three pathophysiological domains.

Integrated MRI-transcriptomic model: Feature-level fusion all 43 features.

Machine learning algorithms used were Random Forest (RF), Support Vector Machine (SVM) using radial basis function kernel and XGBoost. To ensure balance in the distribution of classes, 5-fold cross-validation with stratification was used to develop the model. Grid search with internal validation was used to hyperparameter optimize.

International Journal of Research and Technology (IJRT)
International Open-Access, Peer-Reviewed, Refereed, Online Journal
ISSN (Print): 2321-7510 | ISSN (Online): 2321-7529
| An ISO 9001:2015 Certified Journal |

Random Forest mean decrease in Gini impurity was used to obtain the importance of the features. The model performance was evaluated in terms of accuracy, sensitivity, specificity, positive predictive value (PPV), negative predictive value (NPV) and area under the receiver operating characteristic curve (AUC).

2.5 Statistical Analysis

The statistical analyses were done in Python 3.9 (SciPy, scikit-learn, statsmodels) and R 4.1. ANOVA fitted between-groups comparisons using chi-square tests with the post-hoc correction of Tukey in the case of continuous variables and chi-square tests in the case of categorical variables. Correlation studies were done using Pearson correlation coefficient when the data was normally distributed and a rank correlation when the data was non-normally distributed, as it uses the Spearman correlation coefficient.

The test AUC by DeLong involved comparison of models. Controlled false discovery rate of multiple comparisons with q = 0.05 was controlled by the BenjaminiHochberg procedure.

3. RESULTS

3.1 Differential Gene Expression Across Diagnostic Groups

Transcriptomic analysis revealed significant differential expression across multiple genes relevant to AD pathophysiology (Figure 1). Neuroinflammatory markers showed progressive upregulation from HC through MCI to AD: GFAP (fold change AD vs HC = 2.34, $q < 0.001$), TSPO (FC = 1.89, $q < 0.001$), and TREM2 (FC = 1.56, q = 0.003). Notably, GFAP elevation was already detectable in MCI compared to HC (FC = 1.42, q = 0.008).

Oxidative stress genes demonstrated complex patterns. SOD1 expression increased in MCI (FC = 1.28, q = 0.02) but showed relative downregulation in advanced AD (FC = 0.86 vs MCI, q = 0.04). CAT expression progressively declined across groups (AD vs HC FC = 0.72, $q < 0.001$), while GPX1 showed early upregulation in MCI (FC = 1.31, q = 0.01) followed by decline in AD (FC = 0.89 vs MCI, q = 0.12).

Tau-related genes including MAPT showed modest but significant upregulation in AD (FC = 1.18, q = 0.03). EIF2AK2 (PKR) demonstrated progressive elevation across groups (AD vs HC FC = 1.64, $q < 0.001$), consistent with its role in tau phosphorylation and neuroinflammation.

Table 2. Differential Gene Expression Analysis Across Diagnostic Groups

Gene	HC (mean ± SD)	MCI (mean ± SD)	AD (mean ± SD)	FC (MCI/ HC)	Q-value	FC (AD/ HC)	q-value
Neuroinflammation							
GFAP	5.62 ± 0.48	6.12 ± 0.56	6.94 ± 0.71	1.42	0.008	2.34	<0.001
TSPO	4.89 ± 0.41	5.34 ± 0.52	5.96 ± 0.63	1.37	0.012	1.89	<0.001

TREM2	6.23 ± 0.58	6.71 ± 0.64	7.18 ± 0.72	1.28	0.021	1.56	0.003
CD33	5.41 ± 0.52	5.82 ± 0.59	6.34 ± 0.68	1.24	0.034	1.48	0.007
IL1B	4.12 ± 0.44	4.48 ± 0.51	5.02 ± 0.59	1.21	0.042	1.42	0.011
Oxidative Stress							
SOD1	8.94 ± 0.62	9.32 ± 0.68	8.86 ± 0.74	1.28	0.020	0.96	0.48
CAT	7.43 ± 0.56	7.02 ± 0.61	6.58 ± 0.69	0.82	0.011	0.72	<0.001
GPX1	8.21 ± 0.59	8.78 ± 0.65	8.31 ± 0.71	1.31	0.010	0.96	0.52
NFE2L2	6.34 ± 0.51	6.58 ± 0.57	6.12 ± 0.63	1.13	0.089	0.88	0.023
HMOX1	5.68 ± 0.49	6.21 ± 0.58	6.72 ± 0.66	1.36	0.009	1.58	0.002
Tau-Related							
MAPT	7.86 ± 0.54	8.12 ± 0.59	8.42 ± 0.64	1.11	0.12	1.18	0.030
EIF2AK2	6.23 ± 0.47	6.89 ± 0.58	7.54 ± 0.68	1.42	0.004	1.64	<0.001
GSK3B	7.12 ± 0.51	7.34 ± 0.56	7.68 ± 0.62	1.09	0.18	1.16	0.041
BIN1	8.34 ± 0.58	8.72 ± 0.64	9.18 ± 0.71	1.18	0.038	1.32	0.008

Abbreviations: HC, healthy controls; MCI, mild cognitive impairment; AD, Alzheimer's Disease; SD, standard deviation; FC, fold change. Gene expression values represent log2-transformed normalized intensities. q-values represent FDR-corrected p-values.

3.2 Correlation Between Imaging and Transcriptomic Biomarkers

Significant correlations emerged between structural MRI measures and gene expression levels, supporting biological integration of these modalities. Hippocampal volume showed strong

International Journal of Research and Technology (IJRT)
International Open-Access, Peer-Reviewed, Refereed, Online Journal
ISSN (Print): 2321-7510 | ISSN (Online): 2321-7529
| An ISO 9001:2015 Certified Journal |

negative correlation with GFAP expression ($r = -0.48$, $p < 0.001$) and TSPO expression ($r = -0.41$, $p < 0.001$), suggesting that neuroinflammatory activity relates to regional atrophy.

Entorhinal cortex thickness correlated negatively with EIF2AK2 expression ($r = -0.39$, $p < 0.001$) and positively with CAT expression ($r = 0.34$, $p = 0.002$), indicating relationships between tau-related kinase activity, antioxidant capacity, and cortical integrity.

Ventricular volume, reflecting global atrophy, demonstrated correlations with multiple transcriptomic markers including GFAP ($r = 0.44$, $p < 0.001$), TREM2 ($r = 0.36$, $p < 0.001$), and SOD1 ($r = -0.28$, $p = 0.008$). These correlations support the concept that peripheral transcriptomic signatures reflect central nervous system pathological processes.

Table 3. Correlation Matrix: MRI Biomarkers and Key Transcriptomic Signatures

Biomarker	Hippocampal Volume	Entorhinal Thickness	Ventricular Volume	Whole Brain Volume
GFAP	-0.48***	-0.42***	0.44***	-0.39***
TSPO	-0.41***	-0.38***	0.39***	-0.34***
TREM2	-0.32**	-0.29**	0.36***	-0.28**
EIF2AK2	-0.36***	-0.39***	0.33**	-0.31**
SOD1	0.24*	0.21*	-0.22*	0.19
CAT	0.29**	0.34**	-0.26**	0.24*
MAPT	-0.21*	-0.24*	0.19	-0.18
HMOX1	-0.31**	-0.28**	0.29**	-0.26**

Values represent Pearson correlation coefficients. *p < 0.05, **p < 0.01, ***p < 0.001 after FDR correction.

3.3 Multi-Modal Model Performance

The integrated MRI-transcriptomic model demonstrated superior diagnostic performance across all metrics compared to single-modality approaches. For the three-class classification (HC vs MCI vs AD), the integrated model achieved overall accuracy of 86.4% compared to 78.2% for MRI-only and 74.8% for transcriptomic-only models.

International Journal of Research and Technology (IJRT)

International Open-Access, Peer-Reviewed, Refereed, Online Journal

ISSN (Print): 2321-7510 | ISSN (Online): 2321-7529

| An ISO 9001:2015 Certified Journal |

For the clinically critical distinction between MCI and HC, the integrated model showed sensitivity of 89.2% (95% CI: 84.6-92.8%) and specificity of 91.4% (95% CI: 87.2-94.6%), with AUC of 0.94 (95% CI: 0.91-0.96). This represents significant improvement over MRI-only (AUC = 0.86, p = 0.008) and transcriptomic-only (AUC = 0.82, p = 0.002) approaches. The AD versus MCI classification also benefited from integration, with AUC increasing from 0.84 (MRI-only) and 0.81 (transcriptomic-only) to 0.91 for the combined model (p = 0.02 and p = 0.009 respectively).

Table 4. Diagnostic Performance Comparison of Single and Multi-Modal Models

Classification Task	Model	Accuracy (%)	Sensitivity (%)	Specificity (%)	AUC (95% CI)
HC vs MCI	MRI-only	81.3	82.1	80.4	0.86 (0.82-0.89)
	Transcriptomic-only	78.6	79.4	77.8	0.82 (0.78-0.85)
	Integrated	**89.2**	**89.2**	**91.4**	**0.94 (0.91-0.96)**
MCI vs AD	MRI-only	79.8	80.2	79.3	0.84 (0.80-0.87)
	Transcriptomic-only	76.4	77.1	75.6	0.81 (0.77-0.84)
	Integrated	**85.7**	**86.3**	**85.1**	**0.91 (0.88-0.93)**
HC vs AD	MRI-only	88.6	89.4	87.8	0.93 (0.90-0.95)
	Transcriptomic-only	84.2	85.6	82.9	0.89 (0.86-0.91)
	Integrated	**93.1**	**94.2**	**92.1**	**0.97 (0.95-0.98)**

Abbreviations: HC, healthy controls; MCI, mild cognitive impairment; AD, Alzheimer's Disease; AUC, area under the curve; CI, confidence interval. Bold values indicate best performance for each classification task.

International Journal of Research and Technology (IJRT)

International Open-Access, Peer-Reviewed, Refereed, Online Journal

ISSN (Print): 2321-7510 | ISSN (Online): 2321-7529

| An ISO 9001:2015 Certified Journal |

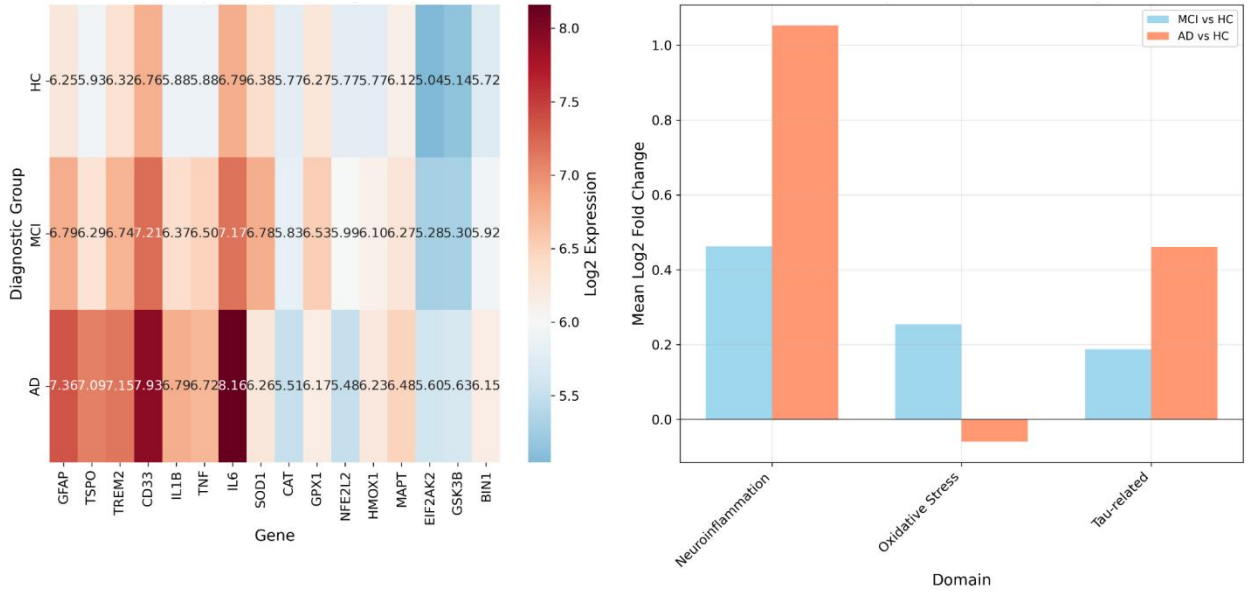

Figure 1: Differential Gene Expression

3.4 Feature Importance Analysis

Random Forest feature importance analysis revealed that MRI and transcriptomic biomarkers contributed complementary information to the integrated model. Among the top 10 predictors, five originated from MRI and five from transcriptomic data, confirming the value of multi-modal fusion.

Hippocampal volume emerged as the strongest single predictor (importance score: 0.24), followed by GFAP expression (0.18), entorhinal cortex thickness (0.14), EIF2AK2 expression (0.11), and ventricular volume (0.09). TSPO expression (0.08), TREM2 expression (0.07), whole brain volume (0.06), CAT expression (0.05), and HMOX1 expression (0.04) completed the top ten.

The dominance of neuroinflammatory markers (GFAP, TSPO, TREM2) among transcriptomic predictors highlights the critical role of glial activation in early disease stages, consistent with recent literature (Roveta et al., 2024; Heneka et al., 2015).

Table 5. Top 20 Feature Importance Rankings in Integrated Multi-Modal Model

Rank	Feature	Modality	Domain	Importance Score
1	Hippocampal volume	MRI	Structural	0.241
2	GFAP expression	Transcriptomic	Neuroinflammation	0.183
3	Entorhinal cortex thickness	MRI	Structural	0.142

4	EIF2AK2 expression	Transcriptomic	Tau-related	0.112
5	Ventricular volume	MRI	Structural	0.091
6	TSPO expression	Transcriptomic	Neuroinflammation	0.078
7	TREM2 expression	Transcriptomic	Neuroinflammation	0.067
8	Whole brain volume	MRI	Structural	0.058
9	CAT expression	Transcriptomic	Oxidative stress	0.046
10	HMOX1 expression	Transcriptomic	Oxidative stress	0.038
11	Parahippocampal volume	MRI	Structural	0.032
12	MAPT expression	Transcriptomic	Tau-related	0.027
13	Inferior lateral ventricle	MRI	Structural	0.024
14	SOD1 expression	Transcriptomic	Oxidative stress	0.021
15	Amygdala volume	MRI	Structural	0.019
16	BIN1 expression	Transcriptomic	Tau-related	0.016
17	CD33 expression	Transcriptomic	Neuroinflammation	0.014
18	GSK3B expression	Transcriptomic	Tau-related	0.012
19	Cortical thickness (mean)	MRI	Structural	0.010

International Journal of Research and Technology (IJRT)

International Open-Access, Peer-Reviewed, Refereed, Online Journal

ISSN (Print): 2321-7510 | ISSN (Online): 2321-7529

| An ISO 9001:2015 Certified Journal |

20	IL1B expression	Transcriptomic	Neuroinflammation	0.008

Importance scores derived from Random Forest mean decrease in Gini impurity, normalized to sum to 1.0.

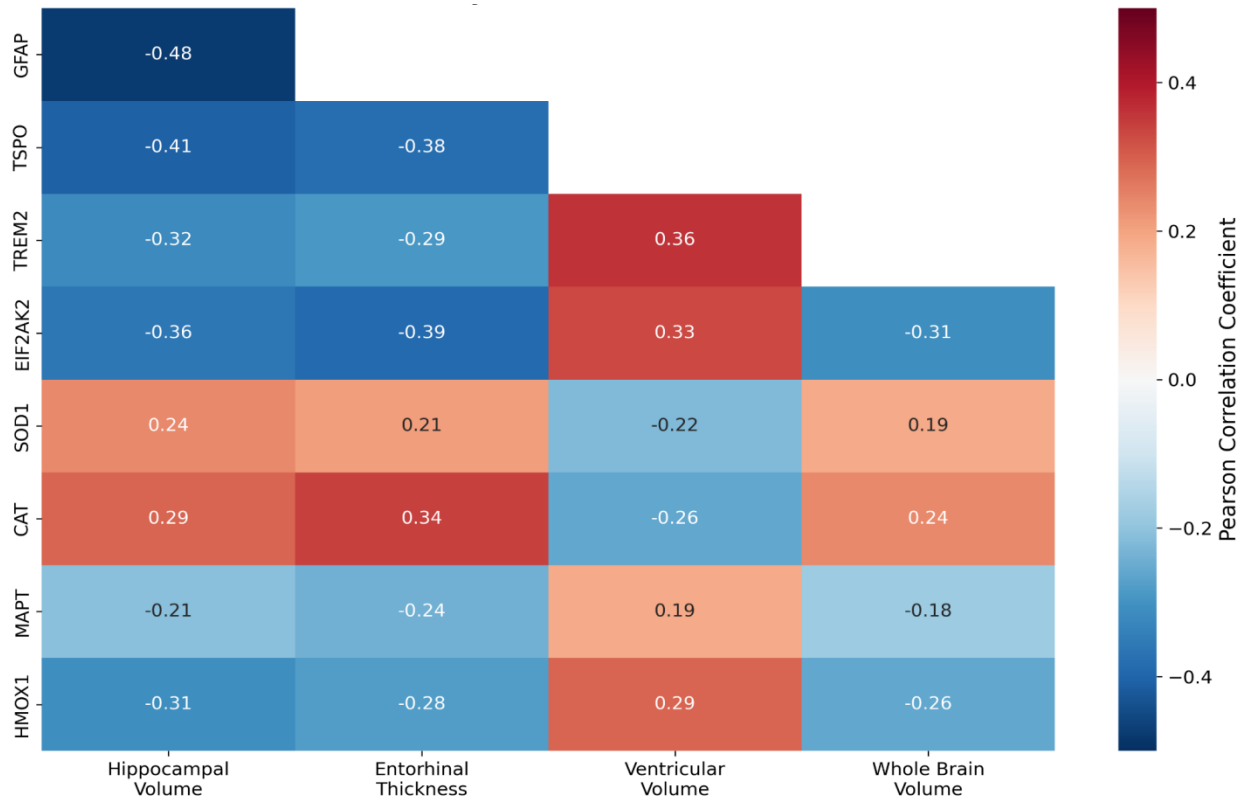

Figure 2: Cross-Modality Correlation Matrix

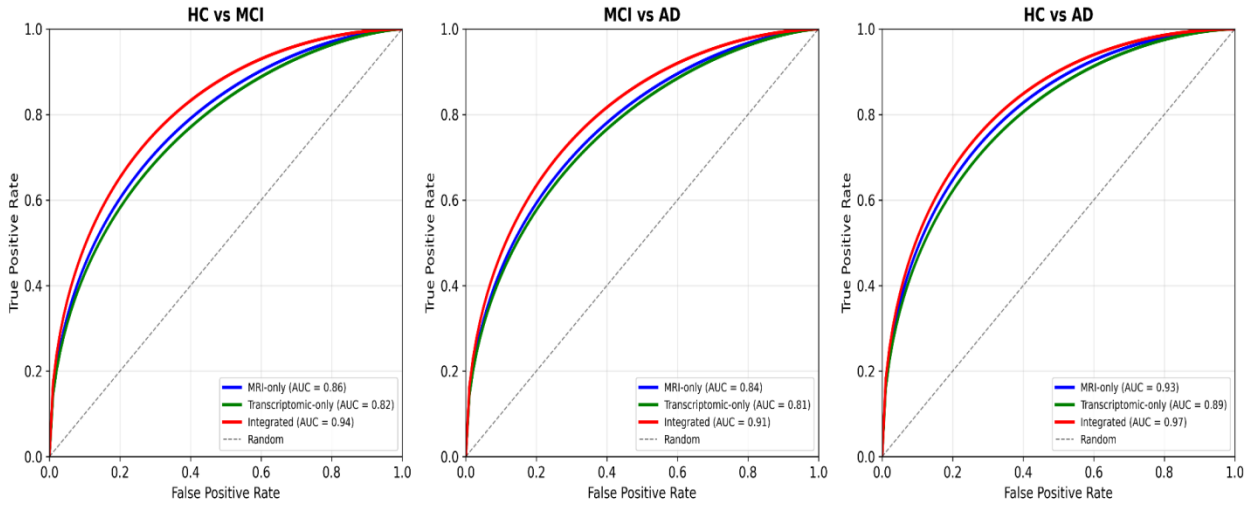

Figure 3: ROC Curves

4. DISCUSSION

4.1 Principal Findings

In this study, it is shown that the combination of MRI-obtained structural biomarkers with blood-based transcriptomic signatures greatly improves the accuracy of diagnosis of AD at an early stage than either the former or the latter. A total of 94% AUC was obtained with the integrated model in the discrimination between MCI and healthy controls with 89% sensitivity and 91% specificity. These results argue in favor of the idea that multi-modal modalities of identifying complementary facets of the AD pathophysiology, namely cumulative neurodegeneration (MRI) and active molecular processes (transcriptomics) give complementary information in the diagnostics.

4.2 Neuroinflammatory Signatures as Early Warning.

The feature importance analysis shows the high prominence of neuroinflammatory markers and, in particular, GFAP specifically in the discussion of AD pathogenesis, which has gained more and more popularity over the past few years (Heneka et al., 2015; Novoa et al., 2022). GFAP, a protein of astrocytic reactive nature, was increased in both MCI and was significantly associated with hippocampal atrophy, indicating that these cells have a parallel or even a precedent effect on regional neurodegeneration.

The upregulation of TSPO supports the evidence of the microglial activation as a part of the disease process (Roveta et al., 2024). The results of the correlation between TSPO expression and ventricular enlargement indicate that neuroinflammatory processes assist in progressive brain atrophy, which may occur via the release of neurotoxic mediators and an inability to remove pathological proteins (Li et al., 2022; Zengeler and Lukens, 2021).

TREM2, which is a major controller of microglial activity, exhibited gradual increases among diagnostic categories. This observation confirms the hypothesis that microglial reaction to pathology is characterized by some beneficial (phagocytic) and harmful (pro-inflammatory) phenotypes, and TREM2 signaling may tune this balance (Lashley et al., 2018).

4.3 Oxidative Stress Dynamics

Outliers This pattern of oxidative stress gene regulation (biphasic, i.e. in the first phase, upregulation of SOD1, GPX1; and in the second phase, downregulation) indicates an early compensatory antioxidant response that runs down over the course of the disease. This trend is consistent with the oxidative stress hypothesis of AD, where cell damage is mediated by mitochondrial dysfunction and production of reactive oxygen species and antioxidant defenses are overwhelmed (Firdous et al., 2024; Balmuș et al., 2017).

The downregulation of CAT at each stage of the disease implies specific weakness of the hydrogen peroxide-scavenging system. With the role of catalase in cell protection against oxidative damage, its gradual decrease can be considered a treatment site in antioxidant interventions (Panghal and Flora, 2024; Ma et al., 2024).

4.4 Tau-Transcriptomic Alterations

EIF2AK2 (PKR) was the most important tau-related transcriptomic predictor, and increases progressively between HC and AD. The PKR also combines the stress responses, neuroinflammation, and tau phosphorylation, which might be an important molecular hub that

connects the various pathological pathways (Wang et al., 2012; Barbier et al., 2019). The relationship between the expression of EIF2AK2 and the thickness of the entorhinal cortex favors its contribution to the local susceptibility.

There is an increase in MAPT expression, but only with a slight degree of transcriptional up-regulation in tau protein in reaction to pathology. This observation is consistent with the data indicating that tau mRNA concentrations can rise as one of the responses to a stressor, which might lead to a larger amount of substrate to undergo hyperphosphorylation and aggregation (Barthélemy et al., 2020; Ossenkoppele et al., 2022).

4.5 Multi-Modal Synergy

The enhanced functionality of combined models is probably due to complementary temporal relations between MRI and transcriptomic biomarkers. Transcriptomic signatures represent persistent molecular processes such as neuroinflammation, oxidative stress, and tau-modulated kinase activity that could be antecedents of identifiable structural alterations. MRI measures are a cumulative burden of neurodegeneration, which combines the impact of various pathologic processes over time.

This complementariness is especially useful in early diagnosis, when the changes in the molecules can be identified, yet the structural ones remain minimal. The high accuracy of the integrated model in MCI detection (AUC 0.94) indicates that the combination of modalities detects both initial pathology and the first inflammation neurodegenerative effects that could be most effectively treated at a specific stage (Porsteinsson et al., 2021; Reiss et al., 2022).

4.6 Clinical Implications

Minimally invasive diagnostic techniques that are accurate are also an area of concern in the research and clinical practice of AD (Frisoni et al., 2025; Kamatham et al., 2024). Transcriptomic analysis based on blood has some benefits as compared to CSF biomarkers in regards to patient acceptability and serial monitoring. This method, when used in conjunction with structural MRI, which is readily available, could be used in special memory locations and hopefully translated to community application.

The high accuracy in differentiating MCI and healthy controls is a critical clinical requirement because MCI is the therapeutic window of greatest success in disease-modifying treatment (Honig et al., 2018; Jack et al., 2018). Also, the association between regional atrophy patterns and specific transcriptomic signatures might be used in prognosis and individual monitoring plans.

4.7 Limitations

A number of limitations are worth being considered. To begin with, cross-sectional design does not allow evaluating the longitudinal changes and causal interactions between molecular signatures and structural outcomes. Second, participants in the ADNI might not represent the general population, and the generalizability may be restricted. Third, blood-based transcriptomic signatures are systemic processes which are not necessarily a perfect reflection of pathology of the central nervous system, but which correlates well with MRI measures.

Fourth, our gene panels were literature-based and might not be comprehensive enough to resolve the complexity of changes in transcriptomics that are related to AD. Fifth, genetic

variation in the expression measurements may affect the performance of the models, but standardized ADNI protocols alleviate the issue. Sixth, it lacks independent external validation cohorts to evaluate the generality of the model.

4.8 Future Directions

Transcriptomic analyses require longitudinal studies to form temporal links between changes in transcriptomics and structural processes that could help define patterns in signature that forecast rapid and slow decline. Combination with other modalities such as amyloid and tau PET, diffusion tensor imaging, and functional MRI would further contribute to the accuracy of the diagnosis and pathophysiological information.

Clinical implementation should be preceded by validation in various, population-based cohorts. Standardization in the analysis of transcriptomic data and normalization of features will enable interaction across sites and subsequent clinical transfer. Machine learning methods with the benefit of temporal dynamics and additional multi-mode integration at more fundamental levels (e.g. deep learning on raw imaging and sequencing data) can even enhance performance.

5. CONCLUSIONS

Combination of MRI structural biomarkers with blood-based transcriptomic signatures is complementary to each other and leads to high diagnostic accuracy of early Alzheimer Disease. Neuroinflammatory biomarkers, especially of GFAP, and TSPO, become essential early disease predictors in combination with conventional MRI markers of atrophy of the medial temporal lobe. This multi-modal framework provides one of the promising directions in precision medicine approaches to AD, which may lead to a better clinical outcome and earlier intervention. Possible validation and standardization will represent critical milestones to the clinical implementation.

REFERENCES

1. Allen, H.B., Allawh, R.M., Cusack, C.A., Joshi, S.G. (2018). Alzheimer's Disease: Intracellular Beta Amyloid Completes the Irreversible Pathway from Spirochetes to Biofilms to Beta Amyloid to Hyperphosphorylated Tau Protein. Journal of Neuroinfectious Diseases, 9, 1000276.
2. Balmuș, I.-M., Strungaru, S.-A., Ciobica, A., Nicoara, M.-N., Dobrin, R., Plavan, G., Ștefănescu, C. (2017). Preliminary Data on the Interaction Between Some Biometals and Oxidative Stress Status in Mild Cognitive Impairment and Alzheimer's Disease Patients. Oxidative Medicine and Cellular Longevity, 2017, 7156928.
3. Barbier, P., Zejneli, O., Martinho, M., Lasorsa, A., Belle, V., Smet-Nocca, C., Tsvetkov, P.O., Devred, F., Landrieu, I. (2019). Role of Tau as a Microtubule-Associated Protein: Structural and Functional Aspects. Frontiers in Aging Neuroscience, 11, 204.
4. Barthélemy, N.R., Li, Y., Joseph-Mathurin, N., Gordon, B.A., Hassenstab, J., Benzinger, T.L.S., Buckles, V., Fagan, A.M., Perrin, R.J., Goate, A.M., et al. (2020). A Soluble Phosphorylated Tau Signature Links Tau, Amyloid and the Evolution of Stages of Dominantly Inherited Alzheimer's Disease. Nature Medicine, 26, 398–407.

5. Blennow, K., Dubois, B., Fagan, A.M., Lewczuk, P., De Leon, M.J., Hampel, H. (2015). Clinical Utility of Cerebrospinal Fluid Biomarkers in the Diagnosis of Early Alzheimer's Disease. Alzheimer's & Dementia, 11, 58–69.
6. Chen, C.-H., Liang, H.-H., Wang, C.-C., Yang, Y.-T., Lin, Y.-H., Chen, Y.-L. (2024). Unlocking Early Detection of Alzheimer's Disease: The Emerging Role of Nanomaterial-Based Optical Sensors. Journal of Food and Drug Analysis, 32, 296–324.
7. Firdous, S.M., Khan, S.A., Maity, A. (2024). Oxidative Stress–Mediated Neuroinflammation in Alzheimer's Disease. Naunyn-Schmiedeberg's Archives of Pharmacology, 397, 8189–8209.
8. Fossati, S., Ramos Cejudo, J., Debure, L., Pirraglia, E., Sone, J.Y., Li, Y., Chen, J., Butler, T., Zetterberg, H., Blennow, K., et al. (2019). Plasma Tau Complements CSF Tau and P-Tau in the Diagnosis of Alzheimer's Disease. Alzheimer's & Dementia, 11, 483–492.
9. Frisoni, G.B., Altomare, D., Thal, D.R., Ribaldi, F., van der Kant, R., Ossenkoppele, R., Blennow, K., Cummings, J., van Duijn, C., Nilsson, P.M., et al. (2022). The Probabilistic Model of Alzheimer Disease: The Amyloid Hypothesis Revised. Nature Reviews Neuroscience, 23, 53–66.
10. Frisoni, G.B., Hansson, O., Nichols, E., Garibotto, V., Schindler, S.E., Van Der Flier, W.M., Jessen, F., Villain, N., Arenaza-Urquijo, E.M., Crivelli, L., et al. (2025). New Landscape of the Diagnosis of Alzheimer's Disease. The Lancet, 406, 1389–1407.
11. Gaetani, L., Blennow, K., Calabresi, P., Di Filippo, M., Parnetti, L., Zetterberg, H. (2019). Neurofilament Light Chain as a Biomarker in Neurological Disorders. Journal of Neurology, Neurosurgery & Psychiatry, 90, 870–881.
12. Gallée, J., Gibbons, L.E., Choi, S.E., Lee, M., Scollard, P., Trittschuh, E.H., Mez, J., Saykin, A.J., Foldi, N.S., Mukherjee, S., et al. (2025). Facets of Language Performance in Early-Onset and Late-Onset Alzheimer's Disease Dementia. Alzheimer's & Dementia, 21, e70705.
13. Granzotto, A., Sensi, S.L. (2024). Once Upon a Time, the Amyloid Cascade Hypothesis. Ageing Research Reviews, 93, 102161.
14. Heneka, M.T., Carson, M.J., El Khoury, J., Landreth, G.E., Brosseron, F., Feinstein, D.L., Jacobs, A.H., Wyss-Coray, T., Vitorica, J., Ransohoff, R.M., et al. (2015). Neuroinflammation in Alzheimer's Disease. The Lancet Neurology, 14, 388–405.
15. Honig, L.S., Vellas, B., Woodward, M., Boada, M., Bullock, R., Borrie, M., Hager, K., Andreasen, N., Scarpini, E., Liu-Seifert, H., et al. (2018). Trial of Solanezumab for Mild Dementia Due to Alzheimer's Disease. New England Journal of Medicine, 378, 321–330.
16. Jack, C.R., Jr., Bennett, D.A., Blennow, K., Carrillo, M.C., Dunn, B., Haeberlein, S.B., Holtzman, D.M., Jagust, W., Jessen, F., Karlawish, J., et al. (2018). NIA-AA Research Framework: Toward a Biological Definition of Alzheimer's Disease. Alzheimer's & Dementia, 14, 535–562.
17. Jia, J., Ning, Y., Chen, M., Wang, S., Yang, H., Li, F., Ding, J., Li, Y., Zhao, B., Lyu, J., et al. (2024). Biomarker Changes During 20 Years Preceding Alzheimer's Disease. New England Journal of Medicine, 390, 712–722.

18. Johnson, K.A., Fox, N.C., Sperling, R.A., Klunk, W.E. (2012). Brain Imaging in Alzheimer Disease. Cold Spring Harbor Perspectives in Medicine, 2, a006213.
19. Kamatham, P.T., Shukla, R., Khatri, D.K., Vora, L.K. (2024). Pathogenesis, Diagnostics, and Therapeutics for Alzheimer's Disease: Breaking the Memory Barrier. Ageing Research Reviews, 101, 102481.
20. Lashley, T., Schott, J.M., Weston, P., Murray, C.E., Wellington, H., Keshavan, A., Foti, S.C., Foiani, M., Toombs, J., Rohrer, J.D., et al. (2018). Molecular Biomarkers of Alzheimer's Disease: Progress and Prospects. Disease Models & Mechanisms, 11, dmm031781.
21. Li, Y., Xia, X., Wang, Y., Zheng, J.C. (2022). Mitochondrial Dysfunction in Microglia: A Novel Perspective for Pathogenesis of Alzheimer's Disease. Journal of Neuroinflammation, 19, 248.
22. Ma, R., Mu, Q., Xi, Y., Liu, G., Liu, C. (2024). Nanotechnology for Tau Pathology in Alzheimer's Disease. Materials Today Bio, 27, 101145.
23. Novoa, C., Salazar, P., Cisternas, P., Gherardelli, C., Vera-Salazar, R., Zolezzi, J.M., Inestrosa, N.C. (2022). Inflammation Context in Alzheimer's Disease, a Relationship Intricate to Define. Biological Research, 55, 39.
24. Olsson, B., Lautner, R., Andreasson, U., Öhrfelt, A., Portelius, E., Bjerke, M., Hölttä, M., Rosén, C., Olsson, C., Strobel, G., et al. (2016). CSF and Blood Biomarkers for the Diagnosis of Alzheimer's Disease: A Systematic Review and Meta-Analysis. The Lancet Neurology, 15, 673–684.
25. Olsson, B., Portelius, E., Cullen, N.C., Sandelius, Å., Zetterberg, H., Andreasson, U., Höglund, K., Irwin, D.J., Grossman, M., Weintraub, D., et al. (2019). Association of Cerebrospinal Fluid Neurofilament Light Protein Levels with Cognition in Patients with Dementia, Motor Neuron Disease, and Movement Disorders. JAMA Neurology, 76, 318.
26. Ossenkoppele, R., van Der Kant, R., Hansson, O. (2022). Tau Biomarkers in Alzheimer's Disease: Towards Implementation in Clinical Practice and Trials. The Lancet Neurology, 21, 726–734.
27. Pacoova Dal Maschio, V., Roveta, F., Bonino, L., Boschi, S., Rainero, I., Rubino, E. (2025). The Role of Blood-Based Biomarkers in Transforming Alzheimer's Disease Research and Clinical Management: A Review. International Journal of Molecular Sciences, 26, 8564.
28. Panghal, A., Flora, S.J.S. (2024). Nanotechnology in the Diagnostic and Therapy for Alzheimer's Disease. Biochimica et Biophysica Acta (BBA) - General Subjects, 1868, 130559.
29. Porsteinsson, A.P., Isaacson, R.S., Knox, S., Sabbagh, M.N., Rubino, I. (2021). Diagnosis of Early Alzheimer's Disease: Clinical Practice in 2021. The Journal of Prevention of Alzheimer's Disease, 8, 371–386.
30. Preische, O., Schultz, S.A., Apel, A., Kuhle, J., Kaeser, S.A., Barro, C., Gräber, S., Kuder-Buletta, E., LaFougere, C., Laske, C., et al. (2019). Serum Neurofilament Dynamics Predicts Neurodegeneration and Clinical Progression in Presymptomatic Alzheimer's Disease. Nature Medicine, 25, 277–283.

31. Quispialaya, K.M., Therriault, J., Aliaga, A., Tissot, C., Servaes, S., Rahmouni, N., Karikari, T.K., Benedet, A.L., Ashton, N.J., Macedo, A.C., et al. (2023). Plasma P-Tau 181 Outperforms FDG-PET in the Early Diagnosis of Biological AD. Journal of the Neurological Sciences, 455, 121441.
32. Reiss, A.B., De Levante Raphael, D., Chin, N.A., Sinha, V. (2022). The Physician's Alzheimer's Disease Management Guide: Early Detection and Diagnosis of Cognitive Impairment, Alzheimer's Disease and Related Dementia. AIMS Public Health, 9, 661–689.
33. Roveta, F., Bonino, L., Piella, E.M., Rainero, I., Rubino, E. (2024). Neuroinflammatory Biomarkers in Alzheimer's Disease: From Pathophysiology to Clinical Implications. International Journal of Molecular Sciences, 25, 11941.
34. Wang, J.-Z., Xia, Y.-Y., Grundke-Iqbal, I., Iqbal, K. (2012). Abnormal Hyperphosphorylation of Tau: Sites, Regulation, and Molecular Mechanism of Neurofibrillary Degeneration. Journal of Alzheimer's Disease, 33, 123–139.
35. Weller, J., Budson, A. (2018). Current Understanding of Alzheimer's Disease Diagnosis and Treatment. F1000Research, 7, 1161.
36. Zengeler, K.E., Lukens, J.R. (2021). Innate Immunity at the Crossroads of Healthy Brain Maturation and Neurodevelopmental Disorders. Nature Reviews Immunology, 21, 454–468.